*Journal of Statistical Physics, Vol. 70, Nos. 1/2, 1993*

# Stochastic Resonance in Paramagnetic Resonance Systems

**L. Gammaitoni,[1] M. Martinelli,[2] L. Pardi,[2] and S. Santucci[1]**

Experimental evidence of the stochastic resonance phenomenon in an electron paramagnetic resonance (EPR) system is reported. The amplitude and phase response of the EPR system operating in bistable conditions are measured for increasing values of the noise intensity. Theoretical predictions based on a simple dynamical model for the relevant system observables are shown to be in good agreement with experimental results.

**KEY WORDS:** Noise; magnetic resonance; nonlinear effects.

## 1. INTRODUCTION

Considerable efforts have been devoted recently to the observation of stochastic resonance (SR) in physical systems. Initially proposed[1, 2] as a possible nonlinear mechanism to explain the periodic recurrence of the earth's ice ages, the SR phenomenon captured the attention of the physics community thanks to its odd character: to date it seems to be the only known method to increase the signal-to-noise ratio of a system response by increasing the intensity of the noise affecting the system.

Since its first proposal, a number of digital and analog simulations[3–5] have been performed in order to check different theoretical models. Despite this large production the experimental observations of SR are quite rare and clear evidence of this phenomenon in *natural* systems is still lacking.[6]

The first observation of SR in a man-made complex apparatus was reported in 1988,[7] occurring in a dye ring laser. Laser systems, due to their well-established nonlinear features, appeared to be the best candidates

[1] Dipartimento di Fisica, Università di Perugia, I-06123 Perugia, Italy.
[2] Dipartimento di Fisica, Università di Pisa, I-56125 Pisa, Italy.



0022-4715/93/0100-0425$07.00/0 

to observe SR. Very recently, however, it has been shown that the electron paramagnetic resonance (EPR) systems, under proper conditions, exhibit bistability phenomena[8] and thus can be employed to study SR.[9] In this paper we report on the observation of the SR phenomenon in these new bistable systems with focus on the amplitude and phase response near the resonance condition. The experimental apparatus and measurement methods are outlined in Section 2. The results thus obtained are presented in Section 3. Finally, in Section 4 comparison between theoretical predictions and experimental results is reported.

## 2. EXPERIMENTAL METHOD

Instabilities and hysteresis phenomena can be obtained in EPR experiments, in analogy with the nonlinear behavior observed earlier in laser systems.

In usual EPR spectroscopy the spectra of paramagnetic samples are studied by placing the sample in a microwave resonant cavity. A microwave oscillator feeds the cavity continuously while a feedback electronic circuit locks the oscillator frequency to the resonant frequency $\nu_c$ of the cavity. In such studies the frequency $\nu$ of the oscillator is kept equal to $\nu_c$ and the static magnetic field $H_0$ is swept in order to vary the Larmor frequency $\nu_0 = \gamma H_0/2\pi$ of the sample ($\gamma$ is the gyromagnetic factor). In standard EPR experiments the amplitude of the wave reflected back from the cavity containing the sample at resonance accounts for the imaginary part $\chi''$ of the sample's paramagnetic susceptibility. In order to realize the effects causing instabilities and hysteresis phenomena observed in the response of the EPR system it is convenient to study the response of the cavity as a function of the frequency $\nu$. In these experiments the static magnetic field $H_0$ is fixed at the value corresponding to the Larmor frequency $\nu_0 = \nu_C$, where $\nu_C$ is the cavity frequency value measured at $H_0 = 0$. Under such conditions and for small samples, the cavity response, measured by detecting the reflected microwave power, exhibits an inverted Lorentzian shape, with a single minimum at $\nu = \nu_C$. In this situation our complex EPR system can be viewed as a two-coupled-oscillator system: the microwave cavity and the spin system. Within this picture one can observe a splitting of the resonance frequency of the whole system into two resonance frequencies, whose separation is a function of the strength of the coupling between the cavity and the spin system. In the presence of a strong coupling, i.e., for a high number of paramagnetic centers, the cavity response exhibits two minima corresponding to two clear-cut values of the frequency $\nu$. Detailed studies of the response function, both experimental and theoretical, clearly explain this phenomenon.[8]

The block scheme of the experimental apparatus employed in our experiment is shown in Fig. 1. Block S represents a standard EPR reflection spectrometer, whose relevant components are the microwave generator, the resonant cavity, and the related circuitry. Block C represents the measurement devices, i.e., the frequency counter employed to measure the frequency $v$ and the power meter employed to measure the cavity response. Block D represents the data acquisition and storage system. Block F represents the feedback system which locks the microwave source frequency to the maximum absorption of the cavity, and block $\sum$ is an electronic adder.

A paramagnetic sample (polypyrrole) is inserted into the resonant cavity and a microwave signal is sent to the cavity. Measurement devices measure the frequency $v$ and the power $P_i$ of the signal from the microwave source and the power $P_r$ of the signal reflected back from the cavity. The reflection coefficient $R(v) = P_r/P_i$ is measured by varying the source frequency. When proper conditions for the EPR system are achieved, the reflection coefficient $R(v)$ shows a shape with two distinct minima located at $v = v_-$ and $v = v_+$ ($v_- < v_+$). In Fig. 2 experimental data for a typical reflection coefficient $R(v)$ in the bistable condition are reported.

The dynamical behavior of the frequency $v$ is driven by the feedback system in both standard EPR experiments and in fixed-field-value experiments. In the stationary condition, $v$ oscillates about the frequency of one of the two minima of the reflection coefficient. Every perturbation which forces the frequency to move away from this position is opposed by a force proportional to the slope of $R(v)$, which operates on the microwave source to restore the minimum position frequency (dynamical stable point). This task is accomplished by means of an electric circuit consisting of a

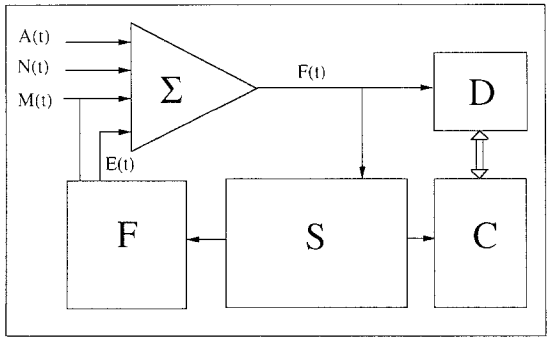


Fig. 1. Block scheme of the experimental apparatus. Block S: EPR spectrometer; block C: measurement devices; block D: data acquisition system; block F: feedback system; block $\sum$: electronic adder.

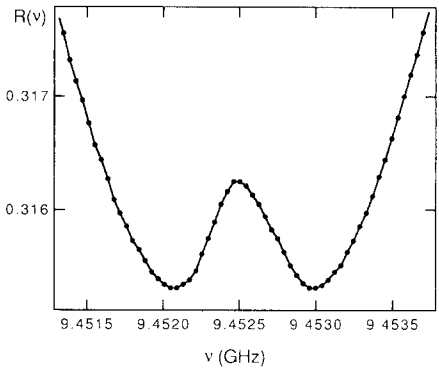


Fig. 2. Bistable cavity reflection coefficient $R(v)$. Units: $y$ axis: arbitrary units; $x$ axis: $10^9$ Hz.

functional multiplier and a low-pass two-pole filter (cutoff frequency $\nu_1 = \omega_1/2\pi = 30$ Hz) which generates an *error signal* $E(t)$ employed to drive the microwave generator. In this way, the working frequency behaves as a dynamical variable subject to a restoring force generated by the feedback system. Instabilities and hysteresis originate just in the action of feedback system, which forces the frequency $v$ from one minimum of $R(v)$ to the other one when $H_0$ is swept across the resonance. External forces, e.g., periodic modulations, can be introduced by adding suitable analog signals on the feedback path by means of the circuit $\sum$.

Furthermore, when the field is constant and $v_0 = v_C$, also in the absence of external causes, the frequency $v$ fluctuates around the stable point due to the unavoidable presence of the noise, which acts as a random force affecting the frequency $v$. If such a random force is of considerable intensity compared to the height of the barrier, $v$ switches any now and then between the minima (Fig. 3). Under these conditions the EPR system shows a noise-driven operating frequency $v(t)$.

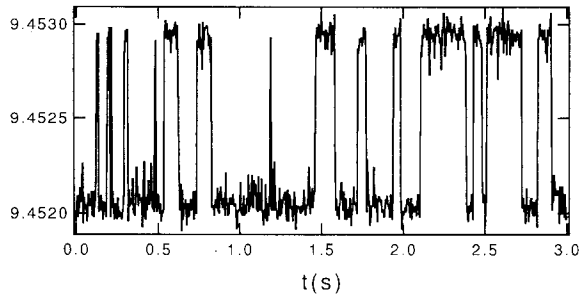


Fig. 3. $v(t)$ time series. Frequency experimental data are sampled with intervals of $5 \times 10^{-3}$ sec.

The sinusoidal signal $A(t) = A\cos(\omega_f t)$ is added to an externally generated wide-band Gaussian noise $\xi(t)$ and to the feedback signal $E(t)$ to produce the *forcing signal* $F(t)$ which drives the microwave generator (Fig. 1). The external modulation signal $M(t)$ requested by the feedback system is also shown in the figure, but plays no role in the low-frequency dynamical behavior in which we are interested because its angular frequency is an order of magnitude greater than $\omega_f$. A useful experimental quantity, $V_E(t)$, is introduced through the relation

$$v[F(t)] = v_c + \mathbf{m}V_E(t) \tag{1}$$

where **m** is the system modulability (frequency/voltage). The dynamical behavior of $V_E(t)$ is thus the same as that of $v(t)$. The *forcing voltage* $V_E(t)$ is sampled at fixed time interval by means of the data acquisition system (block D in Fig. 1) and stored in the system memory. A time series (Fig. 3) consists of a collection of $N$ such experimental samples and is the basic data record used in all the analysis procedures.

## 3. EXPERIMENTAL RESULTS

The SR phenomenon occurs in the bistable EPR system when a periodic signal $A(t)$ is used to drive the *forcing voltage* $V_E(t)$. The amplitude $A$ of $A(t)$ is chosen low enough so that, in the absence of the stochastic force, the operating frequency [*forcing voltage* $V_E(t)$] remains inside one of the wells of the reflection coefficient. When an external noise $\xi(t)$ of suitable intensity is added to $A(t)$, jumps between the two wells occur. A first evidence of SR behavior can be achieved by inspection of the $V_E(t)$ time series for different values of the noise intensity. In Fig. 4 we show three time series sampled for increasing values of the standard deviation $\sigma$ of the Gaussian noise $\xi(t)$ with $A$ and $v$ fixed. In Fig. 4a we observe few rare jumps of $V_E(t)$ between the two equilibrium positions. In this situation the $\sigma$ value is low and thus the escape rate from each well is quite small. No regular pattern in the crossing time sequence is noticeable. On increasing the noise intensity (Fig. 4b), the system matches the SR condition: the time series is characterized by an increased number of jumps and, most importantly, these jumps are synchronous with the periodic driving[9]: a regular pattern of crossings is now apparent. On further increasing the noise intensity (Fig. 4c), this regularity is destroyed and a higher number of jumps occurs randomly in time. In Fig. 5 the stationary distribution density of $V_E(t)$ is shown for the three time series of Fig. 4. The bistable character of $V_E(t)$ is apparent in all the cases. The distribution density corresponding to the top of the barrier increases by increasing $\sigma$, due to the

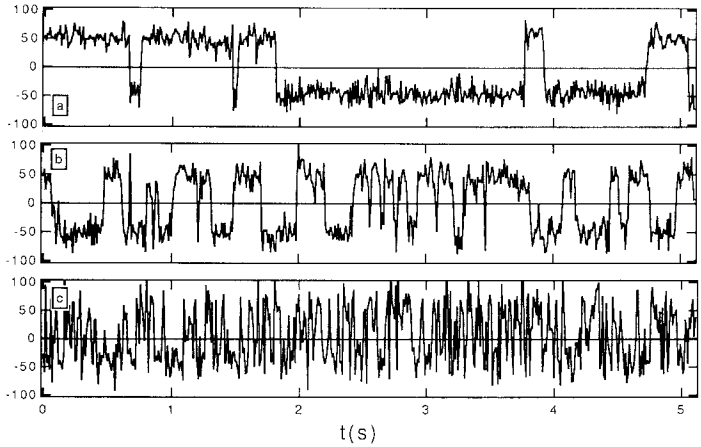


Fig. 4. Time series of $V_E(t)$ for three different values of the noise intensity $\sigma$. Here $A = 5.0 \times 10^{-3}$ V and $\nu_f = 1.9$ Hz. (a) $\sigma = 19.9 \times 10^{-3}$ V; (b) $\sigma = 26.0 \times 10^{-3}$ V; (c) $\sigma = 40.1 \times 10^{-3}$ V. Units: $y$ axis: $10^{-3}$ V; $x$ axis: seconds.

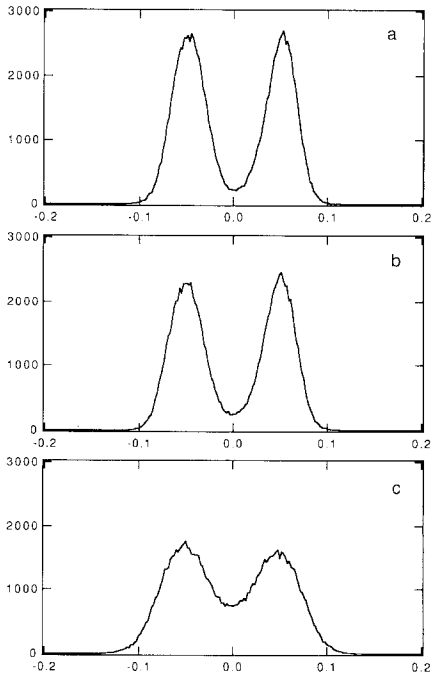


Fig. 5. Stationary distribution density of $V_E(t)$ for the three cases of Fig. 4. Units: $y$ axis: number of sampled points; $x$ axis: volts.

increased probability for the operating frequency [the *forcing voltage* $V_E(t)$] to occupy this region of the reflection coefficient.

A quantitative description of SR requires the choice of suitable observables (order parameters). These observables, following the qualitative description of Fig. 4, must exhibit a nonmonotonic behavior for a monotonic variation of the noise intensity. It is easy to see that this requirement is met by those observables which are directly related to the periodic character of the system response. Further insight can be obtained by looking at the statistics of the residence time distribution of $V_E(t)$ in each well. The average residence time, which is a global feature of the jumping mechanism, decreases by increasing $\sigma$, while the value of the residence time distribution at $T/2 = 1/(2\nu_f)$ [half the period of $A(t)$] increases up to a maximum (SR condition) and then decreases.[10] This last quantity is thus a useful observable for the SR phenomenon.

Usually the periodic character of a time series is analyzed by computing the power spectral density (PSD). In Fig. 6 we report three experimental PSD curves obtained for the same set of parameter values used in cases

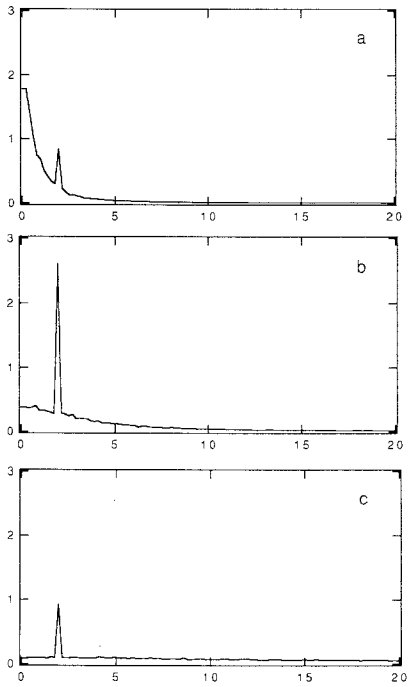


Fig. 6. Power spectra of $V_E(t)$ for the three cases of Fig. 4. Units: $y$ axis: arbitrary units; $x$ axis: hertz.

(a)–(c) of Figs. 4 and 5. All the PSD reported are characterized by a smooth continuous background, accounting for a stochastic dynamics, with a superimposed sharp peak corresponding to the frequency $\nu_f$ of the periodic force $A(t)$. The amplitude of this peak, $S(\nu_f)$, after the subtraction of the continuous background, increases from Fig. 6a to Fig. 6b and decreases from Fig. 6b to Fig. 6c, showing thus a nonmonotonic evolution. The same qualitative behavior is displayed by the signal-to-noise ratio.[7] A quantity strictly related to the PSD is the autocorrelation function (ACF). The ACF of $V_E(t)$ consists of two parts: an exponential decay, which characterizes the correlation behavior at short times and accounts for the stochastic part of the dynamics, and a periodic part, which is typical of the long-time behavior of the ACF. The decay time of the exponential curve monotonically decreases on moving from the case of Fig. 4a to the case of Fig. 4c, while the periodic component, whose amplitude is proportional to the amplitude of the PSD peak $S(\nu_f)$, shows a nonmonotonic evolution in the same range.

In summary, we observe that when the noise intensity matches the proper value the extent of the *periodic character* of $V_E(t)$ reaches a maximum value: this feature is embodied in a number of different physical observables all showing a typical nonmonotonic evolution. In the resonance condition the frequency $\nu$ of the EPR spectrometer is almost exactly driven by the small periodic signal $A(t)$. Most notably, this driving mechanism is characterized by a phase lag $\phi$ between the periodic component of the response $V_E(t)$ and the signal $A(t)$.[2, 11]

Figures 7 and 8 show the evolution of $S(\nu_f)$ and $\phi$ for a wide set of $\sigma^2$ values. The presence of a sharp maximum is apparent in Fig. 7. The $\phi$ curve of Fig. 8 shows instead a monotonic increase from $\phi = -\pi/2$ to $\phi = 0$ and takes the value of about $-\pi/4$ corresponding to the maximum value

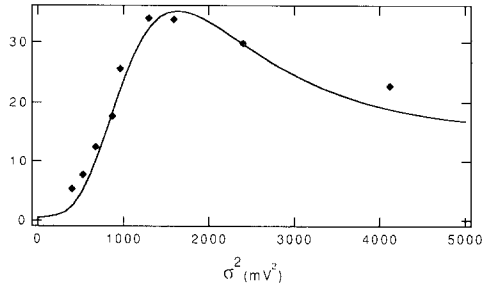


Fig. 7. $S(\nu_f)$ versus $\sigma^2$. Experimental values are displayed along with the theoretical prediction of Eq. (7). Parameter values are as in Fig. 4. Units: $y$ axis: arbitrary units; $x$ axis: $(10^{-3}\ \mathrm{V})^2$.

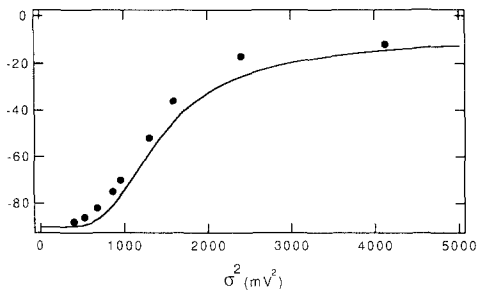


Fig. 8. Dephasing $\phi$ versus $\sigma^2$ for the same configuration as Fig. 7. Experimental values are displayed along with the theoretical prediction of Eq. (8). Units: $y$ axis: degrees; $x$ axis: $(10^{-3}\,\mathrm{V})^2$.

of $S(v_f)$. The observables $\phi$ and $S(v)$ are obtained from time series by computing the cross correlation function (CCF) between the signal $V_E(t)$ and the signal $A(t)$. In the low-noise limit, when the crossing rate becomes very low, the motion inside each well dominates the frequency $v$ dynamics and the EPR system loses its bistable nature. In studying the phase lag quantity in the SR phenomenon we are interested in the interwell motion (jumping dynamics). To avoid spurious effects in the low-noise limit the signal $V_E(t)$ has been filtered through a Schmitt trigger circuit which cancels the low-intensity signals due to intrawell motion. Under this condition the low-noise limit of $\phi$ is $-\pi/2$.

## 4. DISCUSSION

The quantitative description of the experimental results can be obtained by means of a simple one-dimensional model for the frequency $v$ dynamics in the EPR system. Following the arguments sketched in Section 2, is possible to show that the *forcing voltage* $V_E(t)$ obeys the equation of motion

$$\frac{d^2}{dt^2} V_E(t) = -\omega_1 \frac{d}{dt} V_E(t) - \omega_1^2 \frac{d}{dV_E} U(V_E) + \omega_1^2 F_{\text{ext}} \tag{2}$$

with

$$U(V_E) = \tfrac{1}{2} V_E^2 + kR(V_E) \tag{3}$$

Within this picture the power reflection coefficient $R(V_E)$ behaves as a dynamical potential acting on the variable $V_E(t)$. Here $k$ is a coupling constant which depends on the system characteristics. The external forcing terms are represented by $F_{\text{ext}}$. In the case under consideration this term is

the sum of the periodic modulation $A(t)$ and the stochastic force $\xi(t)$ mentioned above. The amplitude of the internal noise sources of the EPR system is much smaller than $\sigma$ and thus will not be considered here. The stochastic force $\xi(t)$ is a Gaussian-distributed random voltage with zero mean and exponential ACF:

$$\langle \xi(t)\, \xi(0) \rangle = \frac{D}{\tau} e^{-|t|/\tau}, \qquad \langle \xi^2 \rangle = \frac{D}{\tau} = \sigma^2$$

The correlation time $\tau$ is about 100 $\mu$sec and is much smaller than any other time constant in the dynamical system under study (white noise approximation). The external force term is thus

$$F_{\text{ext}} = A \cos(\omega t) + \xi(t) \tag{4}$$

with $A < \sigma$. The equation of motion (2) with (4) thus becomes a stochastic differential (Langevin) equation which defines a stochastic process $V_E(t)$. In dealing with the statistical properties of $V_E(t)$ we introduced two kinds of approximations which highly simplify the analytical problem. The mathematical constraints on Eq. (2) required by these approximations can be satisfied by a proper selection of the EPR system characteristics. As a first approximation we considered the overdamped limit of the $V_E(t)$ dynamics. The equation of motion (2) becomes

$$\frac{d}{dt} V_E(t) = \omega_1 \left[ -\frac{d}{dV_E} U(V_E) + F_{\text{ext}} \right]$$

Equation (5) can be used instead of Eq. (2) if

$$\frac{\omega_1}{\omega_E} \approx O(1) \qquad \text{with} \quad \omega_E^2 = \left( \frac{d^2 U}{dV_E^2} \right)_{V_E^0}$$

where $V_E^0$ denotes the absolute value of the symmetric minima of $U(V_E)$. Equation (5) with (4) has been widely employed in recent years to model the SR phenomenon in the overdamped limit.[4, 12–14] Here we will not go through a detailed analysis of this equation. We restrict our interest to a quantitative description of the two chosen system observables $S(v_f)$ and $\phi$. A simple expression for these two quantities can be obtained from the theory in the framework of the adiabatic approximation[4, 15]:

$$S(v_f) = \frac{(V_E^0 A \lambda_1)^2\, \pi}{D^2(\lambda_1^2 + 4\pi^2 v_f^2)} \tag{7}$$

and

$$\phi = -\operatorname{arctg}\left( \frac{2\pi v_f}{\lambda_1} \right) \tag{8}$$

The quantity $\lambda_1$ denotes the first nonzero eigenvalue of the unperturbed Fokker–Planck operator (Kramers rate) associated with Eq. (5).[16]

Sample values of $\lambda_1$ have been obtained by measuring the first passage time of $V_E(t)$ for $A=0$ and different values of the noise intensity: experimental results turn out to be in good agreement with the Kramers theory.[16]

In Figs. 7 and 8 theoretical curves obtained from (7) and (8) are shown as full lines. In spite of the approximations introduced in modeling the EPR system dynamics, the comparison between experimental data and theoretical curves is quite favorable: the main features of both $S(\nu_f)$ and $\phi$ are reproduced with remarkable accuracy.

This result, obtained for the SR phenomenon, seems very promising from a general point of view as well: it suggests the possibility of modeling the EPR system dynamics as a truly nonlinear stochastic dynamics.

## ACKNOWLEDGMENTS

The authors are very indebted to Dr. Fabio Marchesoni for useful discussions and contributions to Section 4.

## REFERENCES

1. R. Benzi, G. Parisi, A. Sutera, and A. Vulpiani, *Tellus* **34**:10 (1982); *SIAM J. Appl. Math.* **43**:565 (1983).
2. C. Nicolis, *Tellus* **34**:1 (1982).
3. S. Fauve and F. Heslot, *Phys. Lett.* **97A**:5 (1983).
4. L. Gammaitoni, F. Marchesoni, E. Menichella-Saetta, and S. Santucci, *Phys. Rev. Lett.* **62**:349 (1989); L. Gammaitoni, E. Menichella-Saetta, S. Santucci, F. Marchesoni, and C. Presilla, *Phys. Rev.* **40A**:2114 (1989).
5. G. Debnath, T. Zhou, and F. Moss, *Phys. Rev.* **39A**:4323 (1989).
6. A. Lontgin, F. Moss, and A. Bulsara, *Phys. Rev. Lett.* **67**:656 (1991).
7. B. McNamara, K. Wiesenfeld, and R. Roy, *Phys. Rev. Lett.* **60**:2626 (1988).
8. M. Giordano, M. Martinelli, L. Pardi, and S. Santucci, *Phys. Rev. Lett.* **59**:327 (1987); M. Cacchiani, M. Giordano, M. Martinelli, L. Pardi, and S. Santucci, *Phys. Rev.* **40A**:5695 (1989).
9. L. Gammaitoni, M. Martinelli, L. Pardi, and S. Santucci, *Phys. Rev. Lett.* **67**:1799 (1991).
10. L. Gammaitoni, Tesi di Dottorato di Ricerca, Pisa (1991).
11. L. Gammaitoni, F. Marchesoni, M. Martinelli, L. Pardi, and S. Santucci, *Phys. Lett.* **158A**:449 (1991).
12. B. McNamara and K. Wiesenfeld, *Phys. Rev.* **39A**:4854 (1988).
13. P. Jung and P. Hanggi, *Europhys. Lett.* **8**:505 (1989); *Phys. Rev.* **41A**:2977 (1990).
14. C. Presilla, F. Marchesoni, and L. Gammaitoni, *Phys. Rev.* **40A**:2105 (1989).
15. H. Gang, G. Nicolis, and C. Nicolis, *Phys. Rev.* **42A**:2030 (1990).
16. H. Risken, *The Fokker–Planck Equation* (Springer-Verlag, Berlin, 1989).